Concentration-dependent polymorphism of insulin amyloid fibrils

Andrius Sakalauskas [1], **Mantas Ziaunys** [1], **Vytautas Smirnovas** [Corresp. 1]

[1] Department of Biothermodynamics and Drug Design, Vilnius University, Life Sciences Center, Institute of Biotechnology, Vilnius, Lithuania

Corresponding Author: Vytautas Smirnovas
Email address: vytautas@smirnovas.info

Protein aggregation into highly structured fibrils has long been associated with several neurodegenerative disorders, such as Alzheimer's or Parkinson's disease. Polymorphism of amyloid fibrils increases the complexity of disease mechanisms and may be one of the reasons for slow progress in drug research. Here we report protein concentration as another factor leading to polymorphism of insulin amyloid fibrils. Moreover, our data suggests that insulin amyloid conformation can self-replicate only via elongation, while seed-induced nucleation will lead to environment-defined conformation of fibrils. As similar observations were already described for a couple of other amyloid proteins, we suggest it to be a generic mechanism for self-replication of different amyloid fibril conformations.

Concentration-dependent polymorphism of insulin amyloid fibrils

Andrius Sakalauskas, Mantas Ziaunys, Vytautas Smirnovas

Institute of Biotechnology, Life Sciences Center, Vilnius University, Vilnius, Lithuania

Corresponding Author:
Vytautas Smirnovas
Sauletekio al. 7, Vilnius, LT-10257, Lithuania

Email address: vytautas.smirnovas@bti.vu.lt

Abstract

Protein aggregation into highly structured fibrils has long been associated with several neurodegenerative disorders, such as Alzheimer's or Parkinson's disease. Polymorphism of amyloid fibrils increases the complexity of disease mechanisms and may be one of the reasons for slow progress in drug research. Here we report protein concentration as another factor leading to polymorphism of insulin amyloid fibrils. Moreover, our data suggests that insulin amyloid conformation can self-replicate only via elongation, while seed-induced nucleation will lead to environment-defined conformation of fibrils. As similar observations were already described for a couple of other amyloid proteins, we suggest it to be a generic mechanism for self-replication of different amyloid fibril conformations.

Introduction

Protein aggregation into amyloid fibrils has been linked to multiple neurodegenerative disorders, including Alzheimer's, Parkinson's and infectious prion diseases (Chiti and Dobson 2017; Knowles, Vendruscolo, and Dobson 2014), which affect tens of millions of people worldwide and is predicted to become even more prominent as the average human lifespan continues to increase (Isik 2010). Matters are further complicated by the fact that very few drugs have reached stage four of clinical trials and no efficient treatment or cure is available (Cummings et al. 2019; Mehta et al. 2017). One of the main reasons for such limited progress in the development of potential cures may be the complexity of fibril formation mechanisms (Meisl et al. 2017), as well as polymorphism of amyloid aggregates (Stein and True 2014).

Ability of the same protein to adopt distinct pathogenic conformations was first reported in studies of infectious prions and such conformations were referred to as strains (Safar et al. 1998; Collinge and Clarke 2007). Recently strain-like polymorphism was reported for a number of

amyloid proteins both *in vivo* (Lu et al. 2013; Watts et al. 2014; Fändrich et al. 2018; Yamasaki et al. 2019) and *in vitro* (Heise et al. 2005; Paravastu et al. 2008; Debelouchina et al. 2010; Dinkel et al. 2011; Bousset et al. 2013). A number of environmental factors including pH (Sneideris et al. 2015), temperature (Tanaka et al. 2006; Colby et al. 2009), concentration of co-solvents(Dzwolak et al. 2004; Chatani et al. 2012), denaturants (Colby et al. 2009; Cobb et al. 2014) or salts (Morel et al. 2010; Bousset et al. 2013), as well as agitation (Petkova et al. 2005; Ostapchenko et al. 2010) can lead to different conformations of amyloid fibrils. Enormous amounts of data must be collected and analyzed in order to understand the complex effects of environment on polymorphism of amyloids.

Due to its relatively low cost, wide availability and simple aggregation protocols, insulin became one of the most common proteins used to study amyloid fibril formation. Several years ago, we summarized available data on polymorphism of insulin amyloid fibrils and came with the hypothesis that the number of insulin amyloid conformations may be limited to two and the major factor which determines formation of different strains is a shift of the equilibrium between insulin monomers and dimers (oligomers) (Sneideris et al. 2015). Our current data supports the existence of a third conformation of insulin amyloid fibrils and suggests that polymorphism of insulin amyloid fibrils is more complex.

Materials and Methods

Insulin sample preparation

Human recombinant insulin powder (Sigma-Aldrich cat. No. 91077C) was dissolved in a 20% acetic acid solution containing 100 mM NaCl (reaction solution) to a final concentration of 2 mM (11.6 mg/ml). Insulin concentration was determined by measuring the sample's absorbance at 280 nm ε=6335 $M^{-1}cm^{-1}$, M = 5808 Da. Samples for unseeded aggregation kinetic measurements were prepared by diluting the 2 mM stock solution using the reaction solution and 10 mM ThT stock solution to a range of concentrations from 0.2 mM to 1.0 mM (which contained 100 μM of ThT). For seeded aggregation, insulin fibrils prepared from the 0.2 mM and 1.0 mM samples were sonicated for 10 min using Sonopuls 3100 (Bandelin) ultrasonic homogenizer equipped with a MS73 tip (40% power, 30 s sonication/ 30 s rest intervals). The homogenized fibrils were then diluted with the reaction solution and mixed with the 2 mM insulin and 10 mM ThT stock solutions to yield 0.2 mM and 1.0 mM concentration samples containing 100 μM ThT and a range of fibril concentrations (from 5 % to 10^{-6} % of monomer mass).

Aggregation kinetics

Insulin aggregation kinetics were monitored at 60 °C without agitation by measuring ThT fluorescence emission intensity (excitation wavelength - 440 nm, emission - 480 nm) through the bottom of a 96 well non-binding surface plate using Synergy H4 Hybrid Multi-Mode (Biotek) plate reader (readouts were taken every 10 min to minimize plate agitation). For every condition

4 independent measurements were performed. Aggregation half-times (t_{50}) were calculated as the time needed to reach 50% of signal intensity.

Atomic Force Microscopy (AFM)

After kinetic measurements, samples were diluted with the reaction solution to a 50 μM concentration and 20 μL of each was deposited on freshly cleaved mica and incubated for 1 min. Subsequently, samples were rinsed with 1 mL of MilliQ water and dried under gentle airflow. Three-dimensional AFM maps were acquired using a Dimension Icon (Bruker) atomic force microscope operating in tapping mode and equipped with a silicon cantilever Tap300AI-G (40 N m^{-1}, Budget Sensors) with a typical tip radius of curvature of 8 nm. High-resolution (1024 x 1024 pixels) images were acquired. The scan rate was 1 Hz. AFM images were flattened and analyzed using SPIP (Image Metrology).

Fourier-Transform Infrared (FTIR) Spectroscopy

Insulin fibrils were separated from solution by centrifugation at 10 000 g for 30 min and subsequently resuspended in 1 mL of D_2O, the procedure was repeated three times. Then the fibrils were resuspended in 0.2 mL of D_2O and sonicated for 1 min using a MS72 tip (with 20% power and constant sonication). Samples were deposited between two CaF_2 transmission windows separated by 0.05 mm teflon spacers. The FTIR spectra were recorded using Vertex 80v (Bruker) IR spectrometer equipped with a mercury cadmium telluride detector, at room temperature under vacuum (~2 mBar) conditions. 256 interferograms of 2 cm^{-1} resolution were averaged for each spectrum. Spectrum of D_2O was subtracted from the spectrum of each sample. All spectra were normalized to the same area of amide I/I' band (1700-1595 cm^{-1}). All data processing was performed using GRAMS software.

Results

Fibril formation at different concentrations

Aggregating a range of insulin concentrations in 20% acetic acid with 100 mM NaCl at 60 °C without agitation reveals a typical kinetic curve pattern, where an increasing insulin concentration leads to shorter aggregation times (Fig. 1A). However, we observe an uneven ratio distribution between ThT fluorescence emission intensities and final fibril concentrations (Fig. 1B). As the concentration of insulin in the sample increases, this ratio shifts ten-fold, indicating either a higher quantum yield or considerably more bound ThT molecules.

FTIR spectra of aggregated samples exhibit maxima in the amide I/I' region at ~1628 cm^{-1} with the shoulder at ~1641 cm^{-1}, and a small band outside of the amide I/I' region at ~1729 cm^{-1} (Fig. 1C), which is very similar to previously reported insulin fibrils formed in phosphate buffer at pH≤2 [Sneideris2015]. However, minor concentration-dependent differences can be observed

(Fig. 1C and D). Spectra of fibrils, formed at lower insulin concentrations have a pronounced shoulder at 1641 cm^{-1}, while a minor band at 1620 cm^{-1} appears in second derivative spectra (Fig. 1D) of samples aggregated at higher protein concentrations. The 1.0 mM and 0.8 mM fibril spectra are nearly identical, while 0.6 mM and 0.4 mM spectra appear to be intermediates between 0.8 mM and 0.2 mM, suggesting the existence of two distinct conformations.

Fibril morphology

The morphology of insulin fibrils formed at different concentrations was compared using AFM. We can see far more small and separated aggregates in samples formed at lower insulin concentration (Fig. 2A-E). Analysis of variance (ANOVA) reveals that there is a statistically relevant fibril height difference ($p=0.01$, $n=50$) between the low and high concentration samples (Fig. 2F). Additional AFM images of these conditions are available as supplementary information (Supplementary Fig. S1).

Seeded aggregation

In order to determine whether observed different fibril templates can propagate at unfavorable conditions, a set of seeded aggregation reactions were performed (Fig. 3A-D, Supplementary Fig. S2). In all four cases we observe a fibril-concentration-dependent seeding propensity (Fig. 3E), however, there is an interesting ThT fluorescence distribution, based on the amount and type of seed added (Fig. 3F). When the 0.2 mM-formed fibril conformation is added to 0.2 mM insulin solutions, there are relatively no major differences in the fluorescence intensity at the end of each reaction. The same can be said in the case when the 1.0 mM-formed conformation is added to 1.0 mM insulin solutions. However, when the 0.2 mM-formed conformation is added to 1.0 mM insulin solutions, high seed concentrations yield a low fluorescence intensity, which then rises with decreased amount of seeds, eventually resulting in an intensity comparable to the 1.0 mM-formed conformation. The opposite is observed when 1.0 mM-formed seeds are added to 0.2 mM insulin solutions, where high initial fibril concentrations yield an intensity comparable to the seed conformation (when accounted for fibril concentration at the end of the reaction) and an intensity similar to fibrils formed at 0.2 mM when the seed concentration becomes minimal. In order to further confirm the self-replication ability of both conformations, fibrils formed during seeded aggregation were examined by FTIR and their spectra were compared to the unseeded aggregation fibril spectra (Fig. 4A-D). The results show that when a large concentration of preformed fibrils is added to either 0.2 mM or 1.0 mM insulin solutions, the seed self-replicates and maintains its initial secondary structure. On the other hand, when a low concentration of seed is added, the resulting FTIR spectra are similar to their respective environment conformations, rather than the seed.

Seeded fibril morphology

When large amounts of sonicated aggregates are used, there is minimal difference in the length and distribution of fibrils (Fig. 5A-D), likely due to the large amount of aggregation centers. When the amount of seed used is low, the fibril length and distribution is similar to unseeded

aggregation (Fig. 5E-H). Fibril height distribution reveals a similarity between almost all conditions, except for when 1.0 mM insulin is seeded with low concentrations of either conformation (Fig. 5I), where the height distribution is comparable to unseeded nucleation. Additional AFM images of these conditions are available as supplementary information (Supplementary Fig. S3).

Discussion

The first and most apparent difference between the samples, aggregated at different protein concentrations is their ability to enhance ThT fluorescence. A very similar effect was reported in case of protein-concentration-dependent polymorphism of glucagon amyloid fibrils (Pedersen et al. 2006). A 10-fold increase in ThT binding positions is highly improbable and slightly different fibril size distribution seen in AFM images could not strongly affect the number of binding positions, so a more appropriate explanation could be changes in the fibril's surface, facilitating a different ThT binding mode, as insulin fibrils have been shown to possess more than one way of incorporating ThT molecules (Groenning et al. 2007). Similar differences in ThT fluorescence were observed with different conformations of alpha-synuclein fibrils and attributed to the different binding of ThT molecules (Sidhu et al. 2018), so we can hypothesize that low protein concentration leads to different conformation of insulin amyloid fibrils.

Protein-concentration-dependent polymorphism of insulin amyloid fibrils is supported also by different FTIR spectra. In fact, spectral differences are rather minor in comparison to the ones observed between spectra of previously reported insulin conformations (Dzwolak et al. 2004; Sneideris et al. 2015), but the hallmark of each spectrum is conserved in seeding experiments (Fig. 4A and B), which supports the hypothesis of different amyloid conformations. Comparison of FTIR spectra to the previously reported data (Sneideris et al. 2015) suggests that fibril conformation formed at higher insulin concentration is the same as previously reported, while the one formed at lower concentration fall out of the previously proposed scheme (Sneideris et al. 2015).

Atomic force microscopy data does not add much of information. It seems that average size of spontaneously formed fibrils slightly increases with higher protein concentration (Fig. 2), but this effect does not depend on the type of seeds (Fig. 5).

Currently we are aware of two mechanisms of seed-induced aggregation. One is amyloid fibril elongation via attachment and refolding of protein molecules at seed fibril ends, another one is formation of new aggregation nuclei catalyzed by the surface of seeds (often referred as secondary nucleation (Meisl et al. 2016)). Previously we have demonstrated that in case of cross-seeding of different environment-induced conformations of prion protein amyloid fibrils, the conformational template can self-propagate only via elongation mechanism, while surface induced nucleation only speeds up the aggregation process, but the conformation is defined by the environment conditions (Sneideris, Milto, and Smirnovas 2015). Recently similar observations were reported on amyloid beta (Brännström et al. 2018) and alpha synuclein (Peduzzo, Linse, and Buell 2019). Our cross-environment seeding data on insulin follows the

same path. With higher amount of seeds the aggregation kinetic curves are exponential which means that the majority of the protein is aggregated via elongation of seeds – in such case the final relative ThT fluorescence intensity and FTIR spectra of seeds and final aggregates are very similar. Lowering the amount of seeds leads to sigmoid kinetic curves which means that the majority of the protein is aggregated via new-formed nuclei and seeds are mainly employed as catalyzers – in such case the final relative ThT fluorescence intensity and FTIR spectra of seeds and final aggregates are different.

Conclusions

Generally, in the seeded growth experiment of amyloid fibrils one expects self-replication of seed conformation. Here we showed that such expectations are valid only at certain circumstances – amyloid fibrils self-replicate their conformation only via elongation, else the conformation of aggregates is environment-dependent. As similar conclusions were previously derived in studies of prion protein, amyloid beta, and alpha-synuclein, there may be enough data to consider it as a general way for self-replication of different amyloid fibril conformations.

209

210 References

211 Bousset, Luc, Laura Pieri, Gemma Ruiz-Arlandis, Julia Gath, Poul Henning Jensen, Birgit
212 Habenstein, Karine Madiona, Vincent Olieric, Anja Böckmann, Beat H. Meier, Ronald
213 Melki. 2013. "Structural and Functional Characterization of Two Alpha-Synuclein Strains."
214 *Nature Communications* 4. https://doi.org/10.1038/ncomms3575.

215 Brännström, Kristoffer, Tohidul Islam, Anna L. Gharibyan, Irina Iakovleva, Lina Nilsson, Cheng
216 Choo Lee, Linda Sandblad, Annelie Pamrén, and Anders Olofsson. 2018. "The Properties
217 of Amyloid-β Fibrils Are Determined by Their Path of Formation." *Journal of Molecular*
218 *Biology* 430 (13): 1940–49. https://doi.org/10.1016/j.jmb.2018.05.001.

219 Chatani, Eri, Hisashi Yagi, Hironobu Naiki, and Yuji Goto. 2012. "Polymorphism of β 2 -
220 Microglobulin Amyloid Fibrils Manifested by Ultrasonication-Enhanced Fibril Formation
221 in Trifluoroethanol." *Journal of Biological Chemistry* 287 (27): 22827–37.
222 https://doi.org/10.1074/jbc.M111.333310.

223 Chiti, Fabrizio, and Christopher M. Dobson. 2017. "Protein Misfolding, Amyloid Formation, and
224 Human Disease: A Summary of Progress Over the Last Decade." *Annual Review of*
225 *Biochemistry* 86 (1): 27–68. https://doi.org/10.1146/annurev-biochem-061516-045115.

226 Cobb, Nathan J., Marcin I. Apostol, Shugui Chen, Vytautas Smirnovas, and Witold K. Surewicz.
227 2014. "Conformational Stability of Mammalian Prion Protein Amyloid Fibrils Is Dictated
228 by a Packing Polymorphism within the Core Region." *Journal of Biological Chemistry* 289
229 (5): 2643–50. https://doi.org/10.1016/j.jmb.2010.05.051.

230 Colby, David W., Kurt Giles, Giuseppe Legname, Holger Wille, Ilia V. Baskakov, Stephen J.
231 DeArmond, and Stanley B. Prusiner. 2009. "Design and Construction of Diverse
232 Mammalian Prion Strains." *Proceedings of the National Academy of Sciences* 106 (48):
233 20417–22. https://doi.org/10.1073/pnas.0910350106.

234 Collinge, John, and Anthony R. Clarke. 2007. "A General Model of Prion Strains and Their
235 Pathogenicity." *Science* 318 (5852): 930–36. https://doi.org/10.1126/science.1138718.

236 Cummings, Jeffrey, Garam Lee, Aaron Ritter, Marwan Sabbagh, and Kate Zhong. 2019.
237 "Alzheimer's Disease Drug Development Pipeline: 2019." *Alzheimer's & Dementia:*
238 *Translational Research & Clinical Interventions* 5: 272–93.
239 https://doi.org/10.1016/j.trci.2019.05.008.

240 Debelouchina, Galia T., Geoffrey W. Platt, Marvin J. Bayro, Sheena E. Radford, and Robert G.
241 Griffin. 2010. "Magic Angle Spinning NMR Analysis of β 2 -Microglobulin Amyloid
242 Fibrils in Two Distinct Morphologies." *Journal of the American Chemical Society* 132 (30):
243 10414–23. https://doi.org/10.1021/ja102775u.

244 Dinkel, Paul D., Ayisha Siddiqua, Huy Huynh, Monil Shah, and Martin Margittai. 2011.
245 "Variations in Filament Conformation Dictate Seeding Barrier between Three- and Four-
246 Repeat Tau." *Biochemistry* 50 (20): 4330–36. https://doi.org/10.1021/bi2004685.

247 Dzwolak, Wojciech, Vytautas Smirnovas, Ralf Jansen, and Roland Winter. 2004. "Insulin Forms

Amyloid in a Strain-Dependent Manner: An FT-IR Spectroscopic Study." *Protein Science* 13 (7): 1927–32. https://doi.org/10.1110/ps.03607204.

Fändrich, M., S. Nyström, K. P. R. Nilsson, A. Böckmann, H. LeVine, and P. Hammarström. 2018. "Amyloid Fibril Polymorphism: A Challenge for Molecular Imaging and Therapy." *Journal of Internal Medicine* 283 (3): 218–37. https://doi.org/10.1111/joim.12732.

Groenning, Minna, Mathias Norrman, James M. Flink, Marco van de Weert, Jens T. Bukrinsky, Gerd Schluckebier, and Sven Frokjaer. 2007. "Binding Mode of Thioflavin T in Insulin Amyloid Fibrils." *Journal of Structural Biology* 159 (3): 483–97. https://doi.org/10.1016/j.jsb.2007.06.004.

Heise, Henrike, Wolfgang Hoyer, Stefan Becker, Ovidiu C. Andronesi, Dietmar Riedel, and Marc Baldus. 2005. "Molecular-Level Secondary Structure, Polymorphism, and Dynamics of Full-Length -Synuclein Fibrils Studied by Solid-State NMR." *Proceedings of the National Academy of Sciences* 102 (44): 15871–76. https://doi.org/10.1073/pnas.0506109102.

Isik, Ahmet Turan. 2010. "Late Onset Alzheimer's Disease in Older People." *Clinical Interventions in Aging* 5 (October): 307–11. https://doi.org/10.2147/CIA.S11718.

Knowles, Tuomas P J, Michele Vendruscolo, and Christopher M. Dobson. 2014. "The Amyloid State and Its Association with Protein Misfolding Diseases." *Nature Reviews Molecular Cell Biology* 15 (6): 384–96. https://doi.org/10.1038/nrm3810.

Lu, Jun-Xia, Wei Qiang, Wai-Ming Yau, Charles D. Schwieters, Stephen C. Meredith, and Robert Tycko. 2013. "Molecular Structure of β-Amyloid Fibrils in Alzheimer's Disease Brain Tissue." *Cell* 154 (6): 1257–68. https://doi.org/10.1016/j.cell.2013.08.035.

Mehta, Dev, Robert Jackson, Gaurav Paul, Jiong Shi, and Marwan Sabbagh. 2017. "Why Do Trials for Alzheimer's Disease Drugs Keep Failing? A Discontinued Drug Perspective for 2010-2015." *Expert Opinion on Investigational Drugs* 26 (6): 735–39. https://doi.org/10.1080/13543784.2017.1323868.

Meisl, Georg, Julius B Kirkegaard, Paolo Arosio, Thomas C T Michaels, Michele Vendruscolo, Christopher M Dobson, Sara Linse, and Tuomas P J Knowles. 2016. "Molecular Mechanisms of Protein Aggregation from Global Fitting of Kinetic Models." *Nature Protocols* 11 (2): 252–72. https://doi.org/10.1038/nprot.2016.010.

Meisl, Georg, Luke Rajah, Samuel A. I. Cohen, Manuela Pfammatter, Anđela Šarić, Erik Hellstrand, Alexander K. Buell, Adriano Aguzzi, Sara Linse, Michele Vendruscolo, Christopher M. Dobson, Tuomas P. J. Knowles. 2017. "Scaling Behaviour and Rate-Determining Steps in Filamentous Self-Assembly." *Chemical Science* 8 (10): 7087–97. https://doi.org/10.1039/C7SC01965C.

Morel, Bertrand, Lorena Varela, Ana I. Azuaga, and Francisco Conejero-Lara. 2010. "Environmental Conditions Affect the Kinetics of Nucleation of Amyloid Fibrils and Determine Their Morphology." *Biophysical Journal* 99 (11): 3801–10. https://doi.org/10.1016/j.bpj.2010.10.039.

Ostapchenko, Valeriy G., Michael R. Sawaya, Natallia Makarava, Regina Savtchenko, K. Peter

R. Nilsson, David Eisenberg, and Ilia V. Baskakov. 2010. “Two Amyloid States of the Prion Protein Display Significantly Different Folding Patterns.” *Journal of Molecular Biology* 400 (4): 908–21. https://doi.org/10.1016/j.jmb.2010.05.051.

Paravastu, Anant K., Richard D. Leapman, W.-M. Yau, and Robert Tycko. 2008. “Molecular Structural Basis for Polymorphism in Alzheimer’s -Amyloid Fibrils.” *Proceedings of the National Academy of Sciences* 105 (47): 18349–54. https://doi.org/10.1073/pnas.0806270105.

Pedersen, Jesper Søndergaard, Dantcho Dikov, James L. Flink, Hans Aage Hjuler, Gunna Christiansen, and Daniel Erik Otzen. 2006. “The Changing Face of Glucagon Fibrillation: Structural Polymorphism and Conformational Imprinting.” *Journal of Molecular Biology* 355 (3): 501–23. https://doi.org/10.1016/j.jmb.2005.09.100.

Peduzzo, Alessia, Sara Linse, and Alexander Buell. 2019. “The Properties of α-Synuclein Secondary Nuclei Are Dominated by the Solution Conditions Rather than the Seed Fibril Strain.” *ChemRxiv.* doi:10.26434/chemrxiv.9757778.v1.

Petkova, Aneta T., Richard D Leapman, Zhihong Guo, Wai-Ming Yau, Mark P Mattson, and Robert Tycko. 2005. “Self-Propagating, Molecular-Level Polymorphism in Alzheimer’s Beta-Amyloid Fibrils.” *Science* 307 (5707): 262–65. https://doi.org/10.1126/science.1105850.

Safar, Jiri, Holger Wille, Vincenza Itri, Darlene Groth, Hana Serban, Marilyn Torchia, Fred E. Cohen, and Stanley B. Prusiner. 1998. “Eight Prion Strains Have PrPSc Molecules with Different Conformations.” *Nature Medicine* 4 (10): 1157–65. https://doi.org/10.1038/2654.

Sidhu, Arshdeep, Jonathan Vaneyck, Christian Blum, Ine Segers-Nolten, and Vinod Subramaniam. 2018. “Polymorph-Specific Distribution of Binding Sites Determines Thioflavin-T Fluorescence Intensity in α-Synuclein Fibrils.” *Amyloid* 25 (3): 189–96. https://doi.org/10.1080/13506129.2018.1517736.

Sneideris, Tomas, Domantas Darguzis, Akvile Botyriute, Martynas Grigaliunas, Roland Winter, and Vytautas Smirnovas. 2015. “pH-Driven Polymorphism of Insulin Amyloid-Like Fibrils.” Edited by Byron Caughey. *PLoS One* 10 (8): e0136602. https://doi.org/10.1371/journal.pone.0136602.

Sneideris, Tomas, Katažyna Milto, and Vytautas Smirnovas. 2015. “Polymorphism of Amyloid-like Fibrils Can Be Defined by the Concentration of Seeds.” *PeerJ* 3 (August): e1207. https://doi.org/10.7717/peerj.1207.

Stein, Kevin C., and Heather L. True. 2014. “Prion Strains and Amyloid Polymorphism Influence Phenotypic Variation.” *PLoS Pathogens* 10 (9): e1004328. https://doi.org/10.1371/journal.ppat.1004328.

Tanaka, Motomasa, Sean R. Collins, Brandon H. Toyama, and Jonathan S. Weissman. 2006. “The Physical Basis of How Prion Conformations Determine Strain Phenotypes.” *Nature* 442 (7102): 585–89. https://doi.org/10.1038/nature04922.

Watts, Joel C., Carlo Condello, J. Stohr, Abby Oehler, Joanne Lee, Stephen J. DeArmond, Lars Lannfelt, Martin Ingelsson, Kurt Giles, and Stanley B. Prusiner. 2014. “Serial Propagation

328 of Distinct Strains of A Prions from Alzheimer's Disease Patients." *Proceedings of the*
329 *National Academy of Sciences* 111 (28): 10323–28.
330 https://doi.org/10.1073/pnas.1408900111.

331 Yamasaki, Tritia R., Brandon B. Holmes, Jennifer L. Furman, Dhruva D. Dhavale, Bryant W.
332 Su, Eun-Suk Song, Nigel J. Cairns, Paul T. Kotzbauer, and Marc I. Diamond. 2019.
333 "Parkinson's Disease and Multiple System Atrophy Have Distinct α-Synuclein Seed
334 Characteristics." *Journal of Biological Chemistry* 294 (3): 1045–58.
335 doi:10.1074/jbc.RA118.004471.

336

Figure 1

Concentration-dependent differences of insulin aggregation.

Aggregation kinetics of unseeded insulin in 20% acetic acid with 100 mM NaCl at 60 °C without agitation followed by ThT fluorescence (A), insert shows aggregation kinetics of 0.2 mM insulin. Each kinetic data point is the average of 4 repeats. ThT fluorescence intensity and fibril concentration ratios (B). FTIR absorption (C) and second derivative (D) spectra of insulin fibrils.

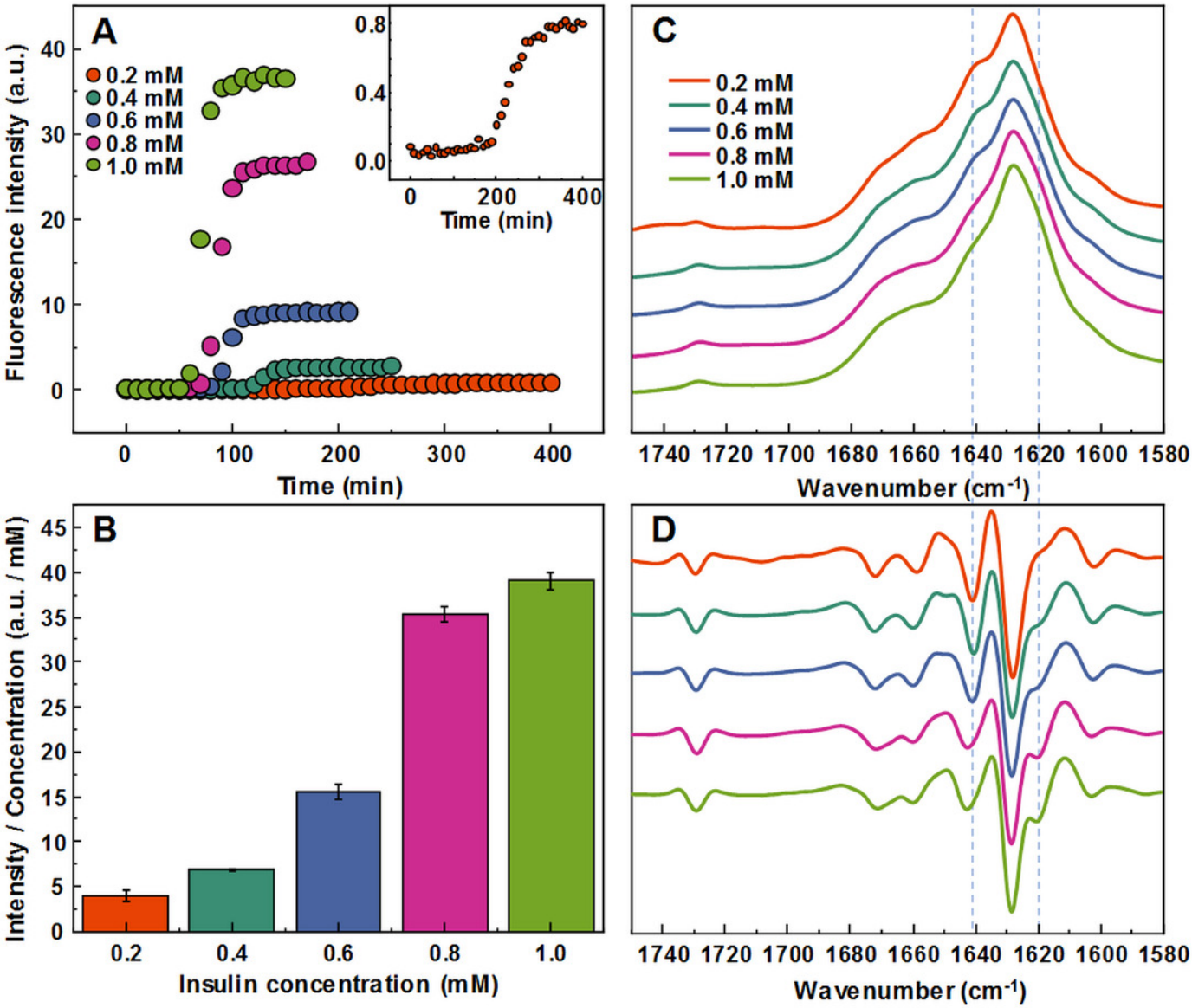
A
0.2 mM
0.4 mM
0.6 mM
0.8 mM
1.0 mM
Fluorescence intensity (a.u.)
Time (min)
B
Intensity / Concentration (a.u. / mM)
Insulin concentration (mM)
C
0.2 mM
0.4 mM
0.6 mM
0.8 mM
1.0 mM
Wavenumber (cm-1)
D
Wavenumber (cm-1)

Figure 2

AFM analysis of insulin fibrils.

Insulin fibrils formed at 0.2 mM (A), 0.4 mM (B), 0.6 mM (C), 0.8 mM (D) and 1.0 mM (E) concentrations. Insulin fibril height distribution with box plots indicating the interquartile range and errors bars are for 1 standard deviation (F). Sample size for each ANOVA test was 50.

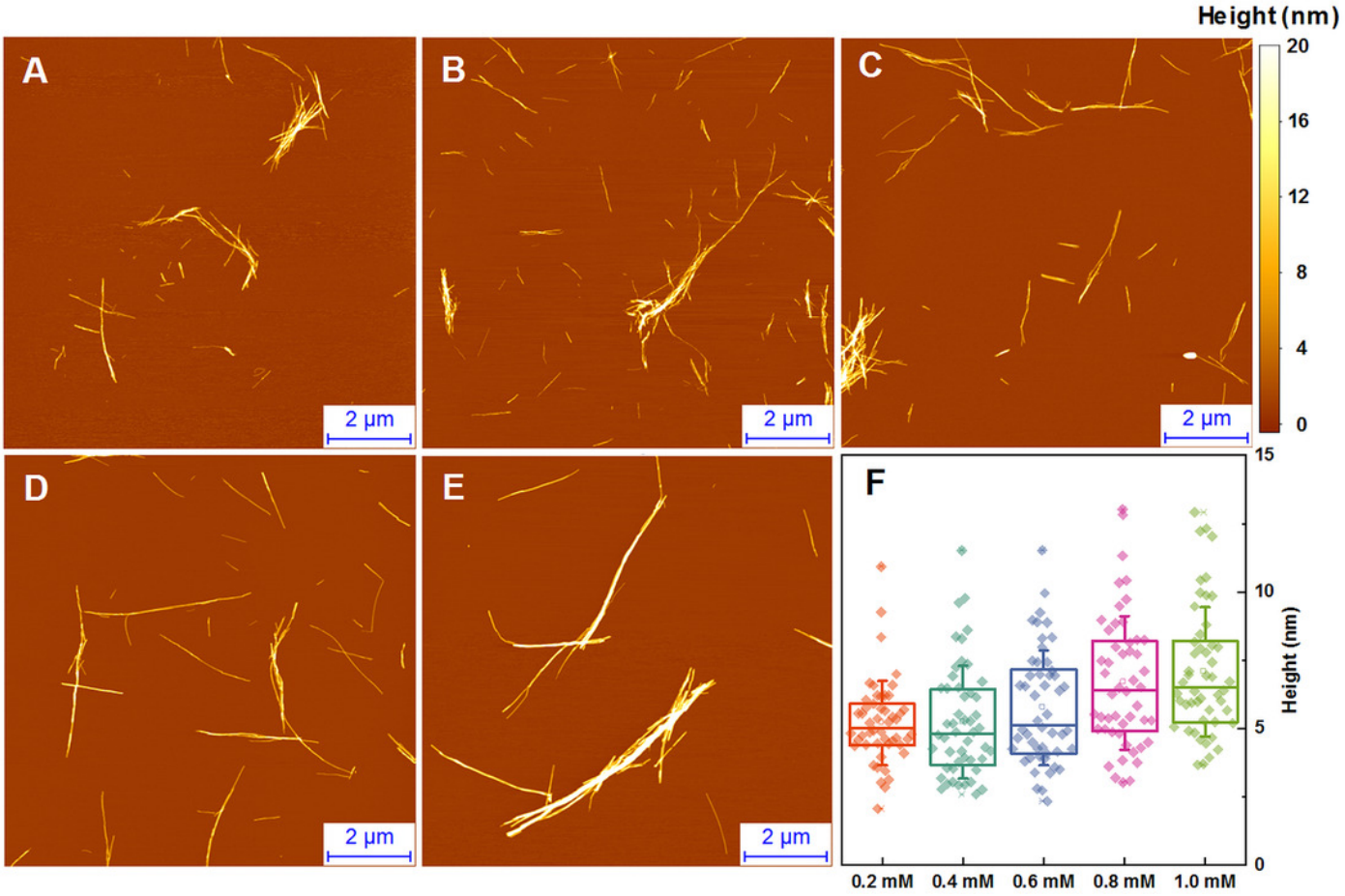

Figure 3

Seeded aggregation of insulin with a range of preformed fibrils.

Aggregation kinetics of insulin where the 0.2 mM-formed conformation is added to 0.2 mM insulin solutions (A), 0.2 mM-formed conformation to 1.0 mM (B), 1.0 mM-formed conformation to 0.2 mM (C) and 1.0 mM-formed conformation to 1.0 mM (D). Aggregation half-time (t_{50}) dependence on concentration and type of seed added (E). ThT fluorescence intensity and fibril concentration ratio dependence on added seed concentration (F). Each data point is the average of 4 repeats.

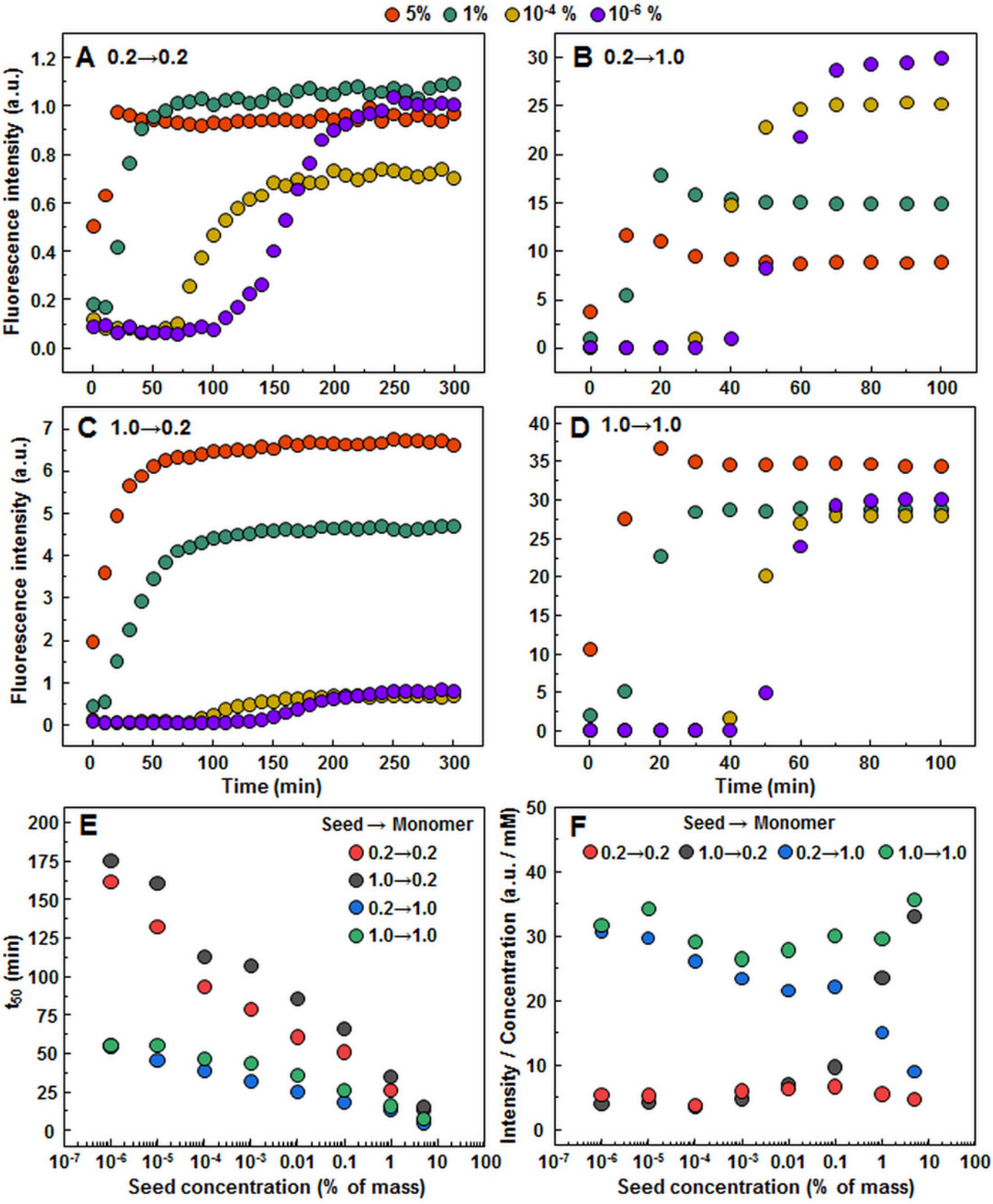
5% 1% 10-4 % 10-6 %
A 0.2→0.2
B 0.2→1.0
C 1.0→0.2
D 1.0→1.0
Fluorescence intensity (a.u.)
Time (min)
E
Seed → Monomer
0.2→0.2
1.0→0.2
0.2→1.0
1.0→1.0
t50 (min)
Seed concentration (% of mass)
F
Intensity / Concentration (a.u. / mM)

Figure 4

FTIR analysis of seeded aggregates.

Absorption and second derivate spectra of insulin fibrils when 5% (A and B respectively) and 0.0001% (C and D respectively) preformed fibrils are added.

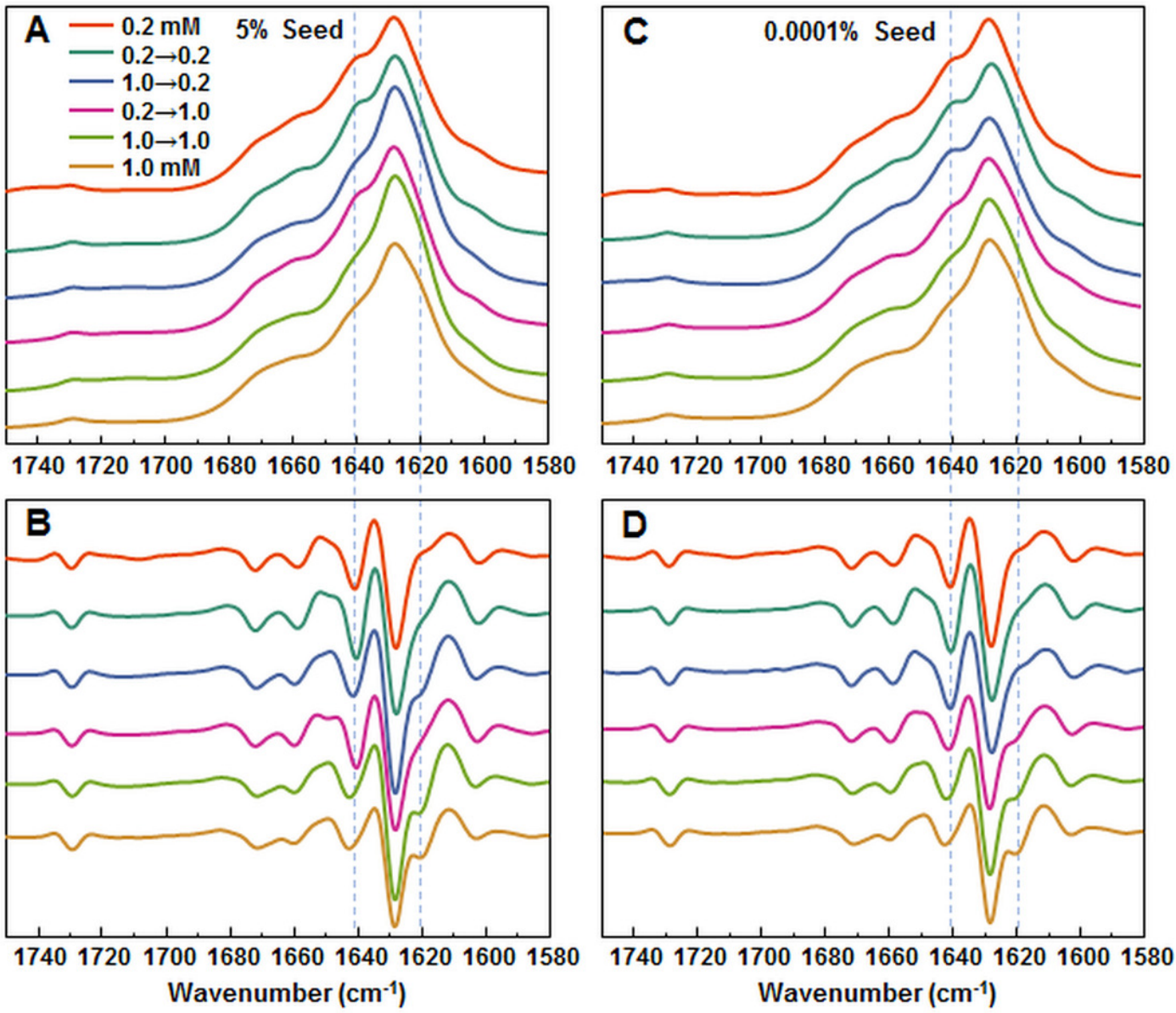

Figure 5

AFM analysis of seeded insulin fibrils.

Insulin fibrils resulting from seeding 0.2 mM insulin with 0.2 mM-formed conformation (A, E), 0.2 mM with 1.0 mM-formed (B, F), 1.0 mM with 0.2 mM-formed (C, G), 1.0 mM with 1.0 mM-formed (D, H) using 5% or 10^{-4} % of preformed fibrils respectively. Insulin fibril height distribution with box plots indicating the interquartile range and errors bars are for 1 standard deviation. Sample size for each ANOVA test was 50.

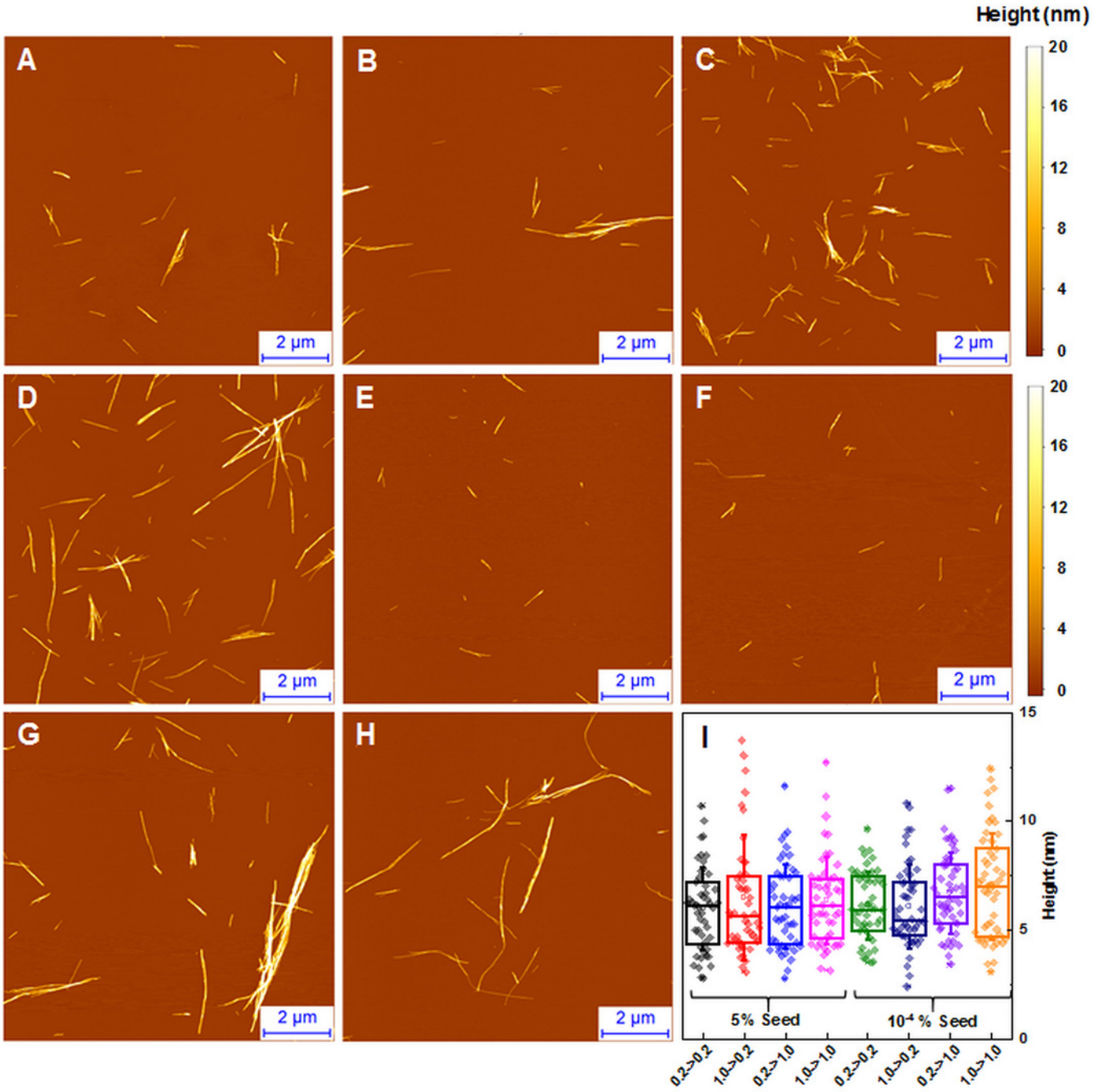
Height (nm)
20
16
12
8
4
0
A
B
C
D
E
F
G
H
2 μm
I
15
10
5
0
Height (nm)
5% Seed
10⁻⁴ % Seed
0.2->0.2
1.0->0.2
0.2->1.0
1.0->1.0
0.2->0.2
1.0->0.2
0.2->1.0
1.0->1.0